TMEM100 induces cell death in non-small cell lung cancer via the activation of autophagy and apoptosis

QIAN HE[1,2*], YILIN DONG[1,3*], YITING ZHU[1], ZHIQIANG DING[4], XINXIN ZHANG[1,5], ZIMENG WANG[6], RONGSHUANG AI[1] and YUJUAN HE[1]

[1]Department of Laboratory Medicine, Key Laboratory of Diagnostic Medicine (Ministry of Education), Chongqing Medical University, Chongqing 400016; [2]Department of Laboratory Medicine, The First People's Hospital of Longquanyi District, Chengdu, Sichuan 610100; [3]Department of Laboratory Medicine, University-Town Hospital of Chongqing Medical University, Chongqing 400030; [4]School of Computer Science, Chongqing Institute of Engineering, Chongqing 401300; [5]Department of Laboratory Medicine, Qilu Hospital of Shangdong University, Qingdao, Shandong 266000; [6]Department of Laboratory Medicine, Chongqing Traditional Chinese Medicine Hospital, Chongqing 400021, P.R. China

Received October 14, 2019; Accepted February 11, 2021

DOI: 10.3892/or.2021.8014

Abstract. Lung cancer is one of the most malignant type of tumors worldwide. Non-small cell lung cancer (NSCLC), which is the most common type of lung cancer, is defined as a distinct disease that exhibits both genetic and cellular heterogeneity. Although in the past two decades significant advances in the treatment of NSCLC have besen performed, the 5-year survival rate of patients with NSCLC remains <20%. Thus, there is an urgent requirement to gain an in-depth understanding of the molecular mechanisms that promote NSCLC development and to identify novel therapeutic targets. In the present study, the gene expression profiles of patients with NSCLC from The Cancer Genome Atlas database were analyzed to determine potential therapeutic targets, and transmembrane protein 100 (TMEM100) was identified as a candidate tumor suppressor. TMEM100 expression level was discovered to be decreased in both NSCLC tissues and cell lines, and it was observed to be negatively associated with the TNM stage and positively associated with prognosis. Moreover, TMEM100 inhibited tumor growth and promoted cell apoptosis in A549 and H460 cells. Mechanistically, TMEM100 was demonstrated to induce autophagy in A549 cells via inhibiting the PI3K/AKT signaling pathway, whereas inhibiting autophagy using bafilomycin A1 significantly enhanced TMEM100-induced apoptosis to compensate for the cell death. In conclusion, these findings suggested that TMEM100 may serve as a tumor suppressor in NSCLC and promote autophagy via inhibiting the PI3K/AKT signaling pathway.

Correspondence to: Professor Yujuan He, Department of Laboratory Medicine, Key Laboratory of Diagnostic Medicine (Ministry of Education), Chongqing Medical University, 1 Yixueyuan Road, Yuzhong, Chongqing 400016, P.R. China
E-mail: heyujuan@cqmu.edu.cn

*Contributed equally

Abbreviations: Baf-A1, bafilomycin A1; CCLE, cancer cell line encyclopedia; DEG, differentially expressed gene; HBE, human bronchial epithelial; IHC, immunohistochemistry; Nrf2, nuclear factor erythroid 2-related factor 2; NSCLC, non-small cell lung cancer; TCGA, The Cancer Genome Atlas; TMEM100, transmembrane protein 100; XAF1, XIAP-associated factor 1

Key words: NSCLC, tumor suppressor, TMEM100, autophagy, apoptosis

Introduction

Lung cancer is the leading cause of cancer-related death in the United States and China, with an approximate 5-year survival rate of ~18% (1). The most common type of lung cancer is non-small cell lung cancer (NSCLC), which accounts for >80% of all cases (2). NSCLC can be further divided into three predominant histological subtypes: Adenocarcinoma, squamous cell carcinoma and large cell carcinoma (2). A total of 70% of patients with lung cancer are diagnosed with advanced stage disease, which poses more challenges for therapy (3). Over the past two decades, the application of various targeted therapies, including the EGFR inhibitor afatinib, and the anaplastic lymphoma kinase inhibitor ceritinib, and immunotherapies, such as the immune checkpoint blocker nivolumab, have resulted in remarkable progress in treating patients with advanced NSCLC; however, drug resistance and a poor response prevented the therapeutic efficacy (4). Therefore, the identification and characterization of novel molecules associated with NSCLC progression is of critical importance for improving both the early diagnosis and treatment of the disease.

Transmembrane protein 100 (TMEM100) transcript was first identified in the mouse genome in 2001 (5). TMEM100 is a 134-amino acid protein, which contains two transmembrane domains at amino acid residues 53-75 and 85-107 (6). It is highly conserved in vertebrates and mammals; however, there is no sequence homology between TMEM100 and any other proteins (6), therefore the biological functions of TMEM100

were further explored in the present study. Previous in-depth studies have revealed that TMEM100 was involved in arterial endothelial differentiation and vascular integrity (6-8), as well as apoptosis (9), enteric nervous system development (10) and persistent pain (11). Interestingly, TMEM100 was demonstrated to be mainly expressed in arterial endothelial cells during the embryonic developmental stage, whereas during adulthood, TMEM100 was most abundantly expressed in the lung, with lower expression in the brain, heart and muscle tissues (7), suggesting that TMEM100 may serve important roles in lung development.

In our previous study, Gene Expression Omnibus datasets (GSE19804, GSE18842, GSE27262 and GSE43458) were downloaded and analyzed to screen differentially expressed genes (DEGs) in NSCLC. Among these DEGs, TMEM100 expression level was significantly decreased in NSCLC tissues compared with normal tissues, which suggested that TMEM100 may serve as a tumor suppressor in NSCLC (data not shown). Recently, TMEM100 has been reported to inhibit tumor progression of NSCLC and hepatocellular carcinoma (12-14). Although the tumor suppressor role of TMEM100 in NSCLC has been revealed, the mechanism of its function is still poorly understood.

Autophagy is an evolutionarily conserved and highly regulated degradation pathway, in which a cell digests its damaged cytoplasmic proteins, macromolecules and organelles to maintain cellular homeostasis (15). The dysregulation of autophagy has been associated with a number of human diseases, including cancer (16). In hepatocellular carcinoma, the levels of autophagy in both aggressive malignant cell lines and tissues from patients with recurrent disease were significantly decreased compared with those of less aggressive cell lines or tissues (17). In addition, Zhang *et al* (18) indicated that DEAD box protein 5 inhibited liver tumor progression by inducing autophagy via interacting with p62. However, other previous studies have reported that the metabolic recycling role of autophagy promoted cancer cell survival under nutrient-deprived conditions (19,20). Furthermore, the deletion of essential autophagy genes, such as Atg7 or Atg5, was demonstrated to impair tumor growth (21). These paradoxical reports have indicated that the role of autophagy in tumor progression may vary depending on the pathological conditions. For example, in NSCLC, nuclear factor erythroid 2-related factor 2 (Nrf2) has been indicated to promote tumorigenic processes by activating autophagy (22), whereas the tumor suppressor casein kinase 1α has been revealed to function as an autophagy inducer to inhibit tumor growth (23), indicating that autophagy serves a contradictory role in NSCLC. However, it remains unknown whether TMEM100, as a potential tumor suppressor, can affect the progression of NSCLC by regulating autophagy.

Therefore, the present study aimed at validating the functions of TMEM100 in different NSCLC cell lines and exploring the potential mechanism of TMEM100 in NSCLC progression. TMEM100 expression level was observed to be decreased in NSCLC tissues and cell lines, and its expression level was negatively associated with the clinical staging and positively associated with the prognosis of patients. Moreover, the overexpression of TMEM100 inhibited proliferation, whilst promoting apoptosis and autophagy in lung cancer cells. Mechanistically, TMEM100-induced autophagy was, at least partially, mediated by inhibiting the PI3K/AKT signaling pathway, and the inhibition of TMEM100-induced autophagy promoted apoptosis to compensate for the cell death. These findings suggested that TMEM100 may serve essential roles as a tumor suppressor in NSCLC by promoting autophagy via the inhibition of the PI3K/AKT signaling pathway. The findings of the present study may provide novel insights for developing new targeted therapy strategies for NSCLC.

Materials and methods

Analysis of the cancer genome atlas (TCGA) database. Gene expression data and the relevant clinical information of 533 cases with lung adenocarcinoma and 59 cases with normal lung tissue were downloaded from TCGA database (http://cancergenome.nih.gov/).

Analysis of the cancer cell line encyclopedia (CCLE) database. Relative gene expression levels in different NSCLC cell lines, including HCC4006, H1734, H460, H1581, H1975, HCC15, H1092, SW900, H1944, H520, A549, SK-MES-1 and H1299, were downloaded from the online CCLE database (https://portals.broadinstitute.org/ccle).

Analysis of Kaplan-Meier Plotter database. The survival rate of 1,926 patients with lung cancer was analyzed using the online database Kaplan-Meier Plotter (http://kmplot.com/analysis/index.php?p=background). All patients were divided into high and low expression groups according to the median level of TMEM100.

Cell culture. The human NSCLC cell lines, A549 and H460, were purchased from Shanghai GeneChem Co., Ltd. (http://www.genechem.com.cn/). H1299 (cat. no. CL-0165), SK-MES-1 (cat. no. CL-0213) and human bronchial epithelial (HBE) cells (cat. no. CL-0346) from Procell Life Science & Technology Co., Ltd. (https://www.procell.com.cn/) were kindly provided by Professor Bu (School of Basic Medicine, Chongqing Medical University, Chongqing, China). The 293T cell line was purchased from American Type Culture Collection (https://www.atcc.org/). A549 cells were cultured in F-12K medium (HyClone; Cytiva), whereas the other cell lines were cultured in RPMI-1640 medium (Gibco; Thermo Fisher Scientific, Inc.), except for 293T cells, which were cultured in DMEM (HyClone; Cytiva). All culture mediums were supplemented with 10% FBS (Biological Industries), 100 U/ml penicillin and 100 μg/ml streptomycin (HyClone; Cytiva), and cells were maintained at 37˚C in a humidified atmosphere containing 5% CO_2.

Cell transfection. The overexpression plasmid pHBLV-CMV-TMEM100 and the corresponding empty vector were purchased from Hanbio Biotechnology Co., Ltd., and TMEM100 small interfering (si)RNAs were obtained from Shanghai Transheep Bio-Tech Co., Ltd. (http://www.transheep.com/). The following TMEM100 siRNA sequences were used: si-TMEM100-1, 5'-GGGAGUGCACAGCAUUAG ATT-3'; and si-TMEM100-2, 5'-CCUACAGUCUUAAGAUGU ATT-3'. A non-targeting siRNA oligonucleotide (5'-UUCUCC GAACGUGUCACGUTT-3') was used as a control. A total of $3.5x10^5$ A549 and H460 cells were seeded into six-well plates,

followed by transient transfection with 3 μg plasmids and 100 pmol siRNAs at 37˚C using Lipofectamine® 2000 reagent (Invitrogen; Thermo Fisher Scientific, Inc.), according to the manufacturer's instructions. Cells were collected 24 and 48 h after transfection for RNA and protein extraction, respectively.

Lentiviral production. A 2nd generation system was used for lentiviral production. Lentiviruses were produced by co-transfecting 293T cells in 60 mm dishes with 1.5 μg pHBLV-CMV-TMEM100 and two packaging plasmids (1.5 μg psPAX2 and 1.5 μg pMD2.G) using Lipofectamine 2000 reagent. Lentiviruses were harvested following 48 h of transfection, centrifuged at 500 x g at 4˚C for 5 min to remove the cell debris, and filtered through a 0.45-μm membrane (EMD Millipore). A549 cells were infected with lentiviruses at a MOI of 50. A549 cells stably overexpressing TMEM100 were selected by treating the lentivirus-infected cells with 1.5 μg/ml puromycin (Beijing Solarbio Science & Technology Co., Ltd.) for 14 days.

Cell viability assay. A total of $2x10^3$ A549 cells were seeded into 96-well plates with six replicates/group, and cultured for 0, 24, 48 or 72 h continuously. At each time point, 10 μl of Cell Counting Kit-8 (Beijing Solarbio Science & Technology Co., Ltd.) reagent was added into each well and incubated for 2 h at 37˚C. The optical density at 450 nm was measured using a microplate reader. The experiments were repeated in triplicate.

Colony formation assay. A549 cells were plated in a six-well plate at a density of 600 cells/well and incubated for 10 days. The plate was washed with PBS, fixed with 4% paraformaldehyde at room temperature for 15 min and the colonies were stained with 0.5% crystal violet at room temperature for 20 min. The number of colonies containing >50 cells was manually counted under an optical microscope (magnification, x400).

Cell cycle analysis. A total of $3.5x10^5$ A549 cells were seeded into a six-well plate and transfected with 3 μg pHBLV-CMV-TMEM100 plasmid or empty vector for 24 h. A total of $4x10^6$ cells from each group were washed with cold PBS, collected and fixed in 70% alcohol at 4˚C overnight. Cells were treated with RNase A for 30 min at 37˚C and subsequently stained with PI at room temperature for 15 min in the dark. Cell cycle analysis was performed using a CytoFLEX flow cytometer (Beckman Coulter, Inc.) and the results were analyzed by CytExpert software v1.0 (Beckman Coulter, Inc.). The assay was repeated in triplicate.

Flow cytometric analysis of apoptosis. A549 and H460 cells transfected with 3 μg pHBLV-CMV-TMEM100 plasmid or 100 pmol siRNAs were collected and washed twice with cold PBS, then resuspended in 100 μl 1X binding buffer. A volume of 5 μl Annexin V-APC (Tianjin Sanjian Biotechnology Co., Ltd.) and 5 μl DAPI were added, mixed well and incubated at room temperature for 10 min in the dark. Apoptotic cells were analyzed using a CytoFLEX flow cytometer and the results were analyzed by CytExpert software v1.0 (Beckman Coulter, Inc.). The lower right (early apoptosis stage) and upper right quadrants (late apoptosis stage) were counted to assess the apoptosis rate. The assay was repeated in triplicate.

Reverse transcription-quantitative PCR (RT-qPCR). Total RNA of H460, HBE, A549, SK-MES-1 and H1299 cells was extracted using RNAiso Plus (Takara Bio, Inc.). The RNA concentration and purity were measured using a Nanodrop ND-100 spectrophotometer (NanoDrop Technologies; Thermo Fisher Scientific, Inc.). A total of 1 μg RNA was reverse transcribed into cDNA using the PrimeScript™ RT Reagent kit (Takara Bio, Inc.), according to the manufacturer's instructions. qPCR was subsequently performed using the CFX96 real-time PCR detection system (Bio-Rad Laboratories, Inc.) and a TB Green™ Premix Ex Taq™ II kit (Takara Bio, Inc.). The following primer sequences were used for the qPCR: GAPDH forward, 5'-TGC ACCACCAACTGCTTAGC-3' and reverse, 5'-GGCATG GACTGTGGTCATGA-3'; and TMEM100 forward, 5'-TGC TGTGGTTGTCTTCATCG-3' and reverse, 5'-CTCTCC CGTCTCTTGGCTTTC-3'. The following thermocycling conditions were used for the qPCR: Initial denaturation at 95˚C for 5 min; 42 cycles of denaturation at 95˚C for 30 sec, annealing at 55˚C for 30 sec and extension at 72˚C for 30 sec. Relative expression levels were determined using the $2^{-\Delta\Delta Cq}$ method (24) and normalized to GAPDH.

Immunofluorescence analysis. A549 cells were fixed with 4% paraformaldehyde at room temperature for 10 min and washed thrice with PBS. Subsequently, cells were permeabilized with 0.5% Triton X-100 at room temperature for 10 min and blocked with 5% BSA (Amresco, LLC) at 37˚C for 1 h. Cells were incubated with anti-LC3A/B (monoclonal; rabbit anti-human; 1:200; cat. no. 4108; Cell Signaling Technology, Inc.) at 4˚C overnight and with anti-rabbit IgG (H + L) (Alexa Fluor® 594 Conjugate; 1:500; cat. no. 8889S; Cell Signaling Technology, Inc.) at 37˚C for 1 h. Nuclei were stained with DAPI at room temperature for 15 min and stained cells were visualized using a fluorescent microscope (magnification, x400; Nikon Corporation).

Immunohistochemistry (IHC). Paraffin-embedded sections, including 15 cases of NSCLC tissues and benign adjacent non-cancerous tissues, were obtained from the Laboratory of Pathology, The First Affiliated Hospital of Chongqing Medical University (Chongqing, China) from 2016 to 2018. The average age of the patients was 58.87±11.92 years, and males accounted for 66.7% and females for 33.3%. The use of these tissue samples was approved by the Ethics and Research Committees of Chongqing Medical University. Written informed consent was obtained from all participants. The slides were routinely deparaffinized, rehydrated and boiled for antigen retrieval in citric acid buffer (pH 6.0) for 10 min. Subsequently, sections were treated with a mouse/rabbit Streptomyces vitellogenin-Biotin Detection system (cat. no. SP-9000; Beijing Zhongshan Golden Bridge Biotechnology Co., Ltd.), according to the manufacturer's instructions. Finally, the slides were mounted and photographed using an optical microscope (magnification, x400).

Western blotting. Total protein was extracted from A549 and H460 cells using RIPA lysis buffer, containing the protease inhibitor PMSF and a phosphatase inhibitor (all from Beyotime Institute of Biotechnology). Protein concentrations

were determined using a BCA Protein Assay kit (Beyotime Institute of Biotechnology) according to the manufacturer's instructions. A total of 40-50 μg protein/lane were separated via 12% SDS-PAGE. The separated proteins were transferred onto PVDF membranes (EMD Millipore) and blocked with 5% BSA (Amresco, LLC) at 37˚C for 2 h. The membranes were incubated with the following primary antibodies overnight at 4˚C: Anti-TMEM100 (monoclonal; mouse anti-human; 1:500; cat. no. MA5-24949; Invitrogen; Thermo Fisher Scientific, Inc.), anti-BAX (monoclonal; rabbit anti-human; 1:1,000; cat. no. AF1270; Beyotime Institute of Biotechnology), anti-BCL2 (monoclonal; rabbit anti-human; 1:1,000; cat. no. AF1915; Beyotime Institute of Biotechnology), anti-LC3A/B (monoclonal; rabbit anti-human; 1:1,000; cat. no. 4108; Cell Signaling Technology, Inc.), anti-p62 (monoclonal; rabbit anti-human; 1:5,000; cat. no. CY5546; Abways Technology), anti-GAPDH (monoclonal; rabbit anti-human; 1:5,000; cat. no. AF1186; Beyotime Institute of Biotechnology), anti-phosphorylated (p)-PI3K (monoclonal; rabbit anti-human; 1:1,000; cat. no. 4228S; Cell Signaling Technology, Inc.), anti-total (t)-PI3K (monoclonal; rabbit anti-human; cat. no. 4257S; 1:1,000; Cell Signaling Technology, Inc.), anti-p-AKT (monoclonal; rabbit anti-human; 1:1,000; cat. no. 2965S; Cell Signaling Technology, Inc.), anti-t-AKT (monoclonal; rabbit anti-human; 1:1,000; cat. no. 4691S; Cell Signaling Technology, Inc.). Following the primary antibody incubation, membranes were incubated with HRP-conjugated goat anti-rabbit IgG (H + L) (1:10,000; cat. no. 04-15-06; KPL) or HRP-conjugated goat anti-mouse IgG (H + L) (1:10,000; cat. no. 04-18-06; KPL) at 37˚C for 1 h. Protein bands were visualized using Immobilon™ Western HRP Substrate Peroxide solution (EMD Millipore) and a Bio-Rad electrophoresis documentation system.

Agonist and inhibitor treatment. A549 cells were pretreated with 30 μM 740Y-P (MedChemExpress) or 20 μM SC79 (Beyotime Institute of Biotechnology) for 1.5 h at 37˚C, and subsequently transfected with 3 μg pHBLV-CMV-TMEM100 plasmid or empty vector for 24 h. H460 cells were pretreated with 20 μM LY294002 (Beyotime Institute of Biotechnology) for 1.5 h at 37˚C, followed by transfection with 100 pmol siRNA or si-NC for 24 h. A total of 50 nM Bafilomycin A1 (Selleck Chemicals) was added into A549 cells for 2 h at 37˚C prior to transfection of 3 μg pHBLV-CMV-TMEM100 plasmid or empty vector. Control cells received an equal volume of DMSO (Beijing Solarbio Science & Technology Co., Ltd.) and the final concentration of DMSO was <0.1%. Subsequently, protein expression levels were determined by western blotting.

Mouse xenograft experiment. The animal studies were approved by the Institutional Animal Care and Use Committee of Chongqing Medical University (Chongqing, China). A total of 10 female athymic BALB/c nude mice (age, 4-5 weeks old; weight, 16-20 g; n=5 per group) were purchased from Chongqing Medical University and housed in specific pathogen-free conditions at constant temperature (22˚C) and humidity (50-60%) on a 12 h light/dark cycle with free access to food and water. A549 cells transfected with empty vector or the TMEM100 overexpression plasmid in the exponential growth phase were diluted to a density of $5x10^6$ cells/100 μl PBS and the cell suspension was injected subcutaneously into the left axilla of each mouse. The mice were monitored every 3 days. Tumors were allowed to grow to 12 mm diameter. The protocol continued until 30 days following tumor cell injection. All experimental mice were sacrificed by cervical dislocation simultaneously, and tumor sizes and weights were measured.

Statistical analysis. Statistical analysis was performed using GraphPad Prism version 5.0 software (GraphPad Software, Inc.) and data are presented as the mean ± SD. Student's t-test was used to determine the differences between two groups. One-way ANOVA followed by Bonferroni's post hoc test was used for multiple group comparisons. Overall survival was calculated using SPSS version 17 (SPSS, Inc.) with Kaplan-Meier estimate and log-rank test. All experiments were carried out at least three times. $P<0.05$ was considered to indicate a statistically significant difference.

Results

TMEM100 expression levels are decreased in NSCLC specimens and cell lines. To identify the potential role of TMEM100 in NSCLC, the expression levels of TMEM100 were analyzed in human lung cancer tissues from TCGA database. TMEM100 expression level was significantly decreased in NSCLC specimens (n=533) compared with normal lung tissues (n=59; Fig. 1A). Additionally, it was observed that the expression level of TMEM100 exhibited a decreasing trend at more advanced TNM stages of NSCLC (Fig. 1B), demonstrating that the expression level of TMEM100 was negatively associated with the tumor stage. In addition, the association between TMEM100 expression level and the survival of patients in TCGA database was analyzed using SPSS software. It was indicated that the patients with lower TMEM100 expression level had worse overall survival, but there was no statistical significance (Fig. S1A). However, the result from the online database Kaplan-Meier Plotter demonstrated that the survival rate of patients with high expression of TMEM100 was significantly higher than those with low expression of TMEM100 (Fig. S1B), which suggested that the expression level of TMEM100 was positively associated with the prognosis of patients with NSCLC. Furthermore, the expression level of TMEM100 in NSCLC tissues (n=15) and the matched benign adjacent non-cancerous tissues were detected using IHC. The expression level of TMEM100 was indicated to be markedly decreased in NSCLC tissues compared with the adjacent non-cancerous tissues (Fig. 1C), which was consistent with the results of TCGA database. In addition, data from the CCLE database were used to examine the relative expression level of TMEM100 in various NSCLC cell lines. It was revealed that the expressions level of TMEM100 was relatively low in 10 NSCLC cell lines, particularly in the A549, SK-MES-1 and H1299 cell lines, whereas it was relatively high in three NSCLC cell lines, including H460 (Fig. 1D). These results were validated in four NSCLC cell lines (A549, SK-MES-1, H1299 and H460) and one normal lung epithelial cell line (HBE) by RT-qPCR (Fig. 1E). Altogether, these findings suggested that TMEM100 may serve an antitumor role in NSCLC.

TMEM100 inhibits the proliferation of NSCLC cells. To investigate the role of TMEM100 in NSCLC progression,

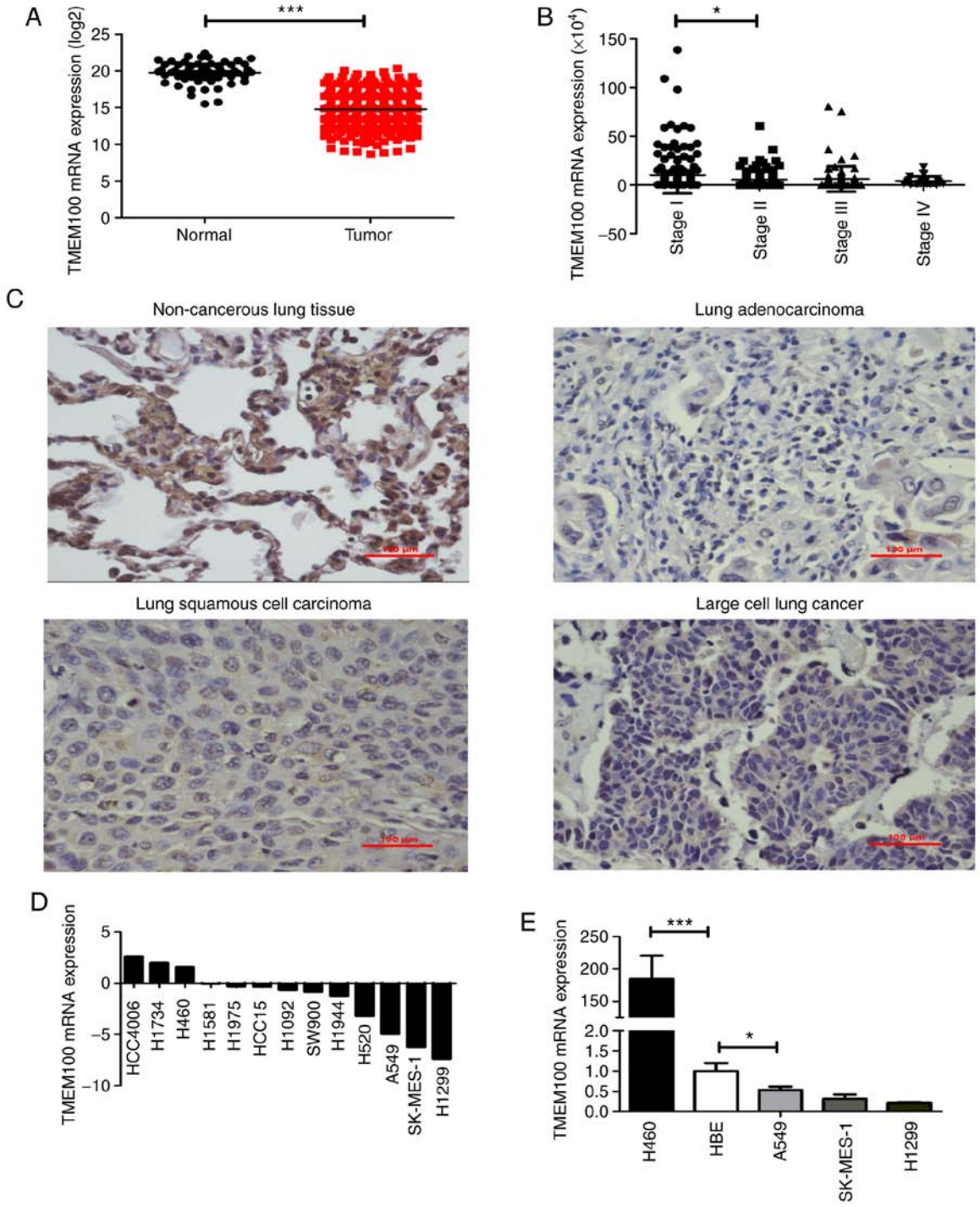

Figure 1. TMEM100 expression level is decreased in NSCLC tissues and cells. (A) Expression level of TMEM100 in lung adenocarcinoma (n=533) and normal lung tissues (n=59) obtained from TCGA database. (B) Expression level of TMEM100 in patients with different stages of lung adenocarcinoma obtained from TCGA database. (C) Immunohistochemical staining of TMEM100 in benign adjacent non-cancerous tissues, lung adenocarcinoma, lung squamous cell carcinoma and large cell lung cancer tissues. Scale bars, 100 μm. (D) Relative expression level of TMEM100 in 13 NSCLC cell lines obtained from the cancer cell line encyclopedia database. (E) Expression level of TMEM100 gene in the normal lung epithelial cell line HBE and NSCLC cell lines. Data are representative of three independent experiments and are presented as the mean ± SD. *P<0.05; ***P<0.001. NSCLC, non-small cell lung cancer; TCGA, The Cancer Genome Atlas; TMEM100, transmembrane protein 100.

TMEM100 was overexpressed in A549 cells and knocked down in H460 cells using a TMEM100 overexpression plasmid and TMEM100 siRNAs, respectively. The transfection efficiency of the overexpression (Fig. 2A and B) and knockdown (Fig. S2A and B) was confirmed by RT-qPCR and western blotting. Subsequently, the effect of TMEM100 on cell proliferation was investigated. As expected, overexpression of TMEM100 significantly inhibited A549 cell proliferation and colony formation (Fig. 2C and D). Furthermore, cell cycle analysis demonstrated that TMEM100 induced cell cycle arrest in the G_1 phase, as ectopic overexpression of TMEM100 significantly increased the percentage of A549 cells in the G_1 phase from 61.20 to 73.63%, but decreased the percentage of cells in the S phase from 28.49 to 13.18% (Fig. 2E). By

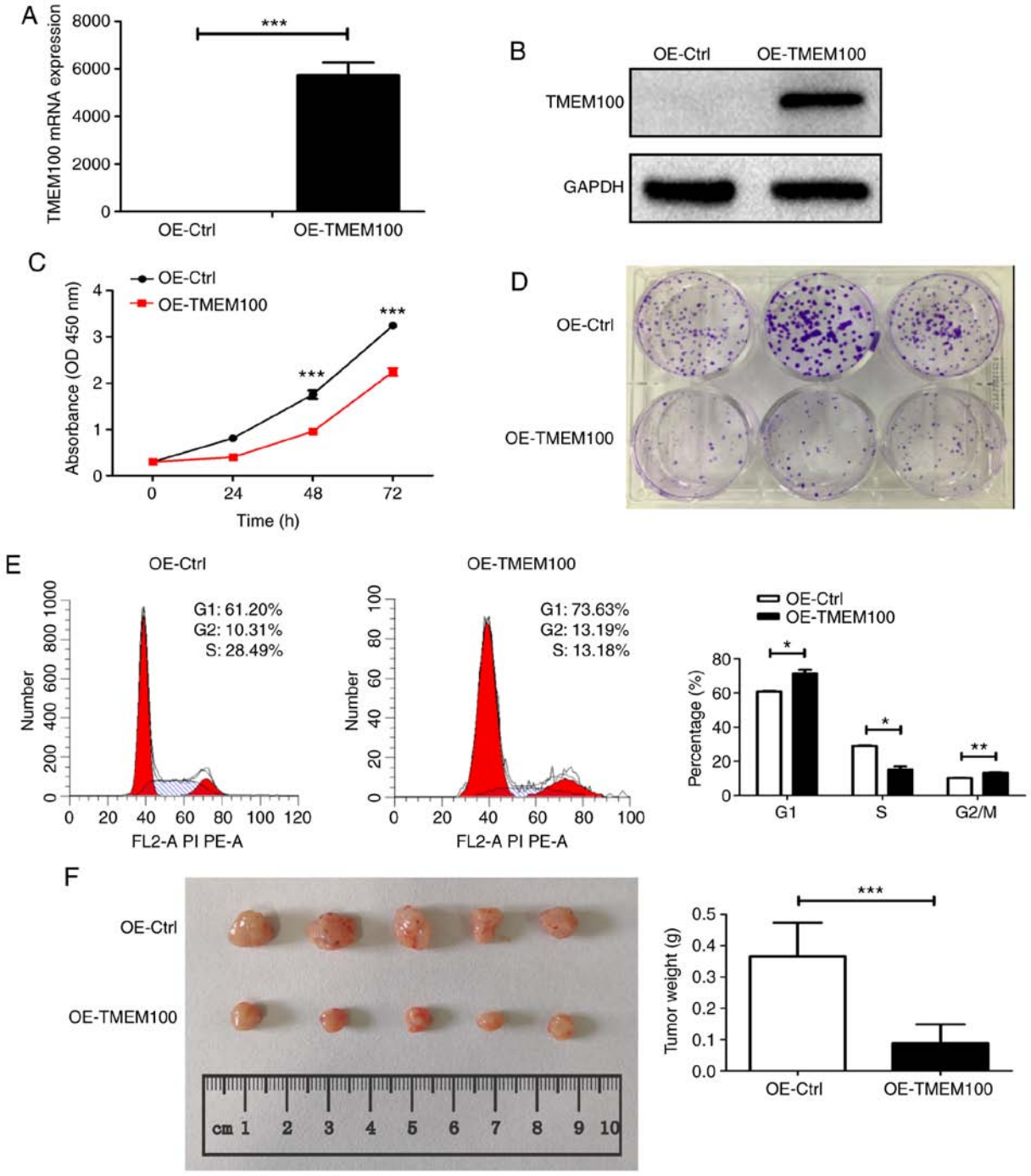

Figure 2. TMEM100 inhibits the growth of non-small cell lung cancer cells. (A) TMEM100 expression level in A549 cells transfected with TMEM100 overexpression plasmid. (B) Expression level of TMEM100 protein in A549 cells transfected with TMEM100 overexpression plasmid. (C) Cell proliferation was analyzed by Cell Counting Kit-8 assay following TMEM100 overexpression. (D) Representative images of colonies formed by A549 cells transfected with TMEM100 overexpression plasmid. (E) Cell cycle analysis of A549 cells upon TMEM100 overexpression. (F) Size and weight of subcutaneous tumors in the TMEM100-overexpression group and control group. Data are representative of three independent experiments and are presented as the mean ± SD. *P<0.05, **P<0.01 and ***P<0.001 vs. OE-TMEM100. TMEM100, transmembrane protein 100; OE, overexpression; OD, optical density; Ctrl, control.

contrast, TMEM100 knockdown enhanced the proliferation of H460 cells (Fig. S2C). To assess the impact of TMEM100 on tumor growth *in vivo*, A549 cells with or without ectopic overexpression of TMEM100 were subcutaneously injected into athymic nude mice. At day 30, tumor size and weight were notably decreased in the TMEM100 overexpression group compared with the control group (Fig. 2F). Thus, both *in vitro* and *in vivo* experiments demonstrated a marked antitumor role of TMEM100 in NSCLC.

TMEM100 promotes apoptosis in NSCLC cells. To investigate the effect of TMEM100 on cell apoptosis, an Annexin V-DAPI apoptosis assay and western blotting, to determine the expression levels of BAX/BCL2, were performed. The early-stage and late-stage apoptotic rate was significantly increased in TMEM100-overexpressing cells compared with control cells (Fig. 3A), suggesting that ectopic overexpression of TMEM100 may promote apoptosis in A549 cells. Consistently, the expression level of the pro-apoptotic protein BAX was increased

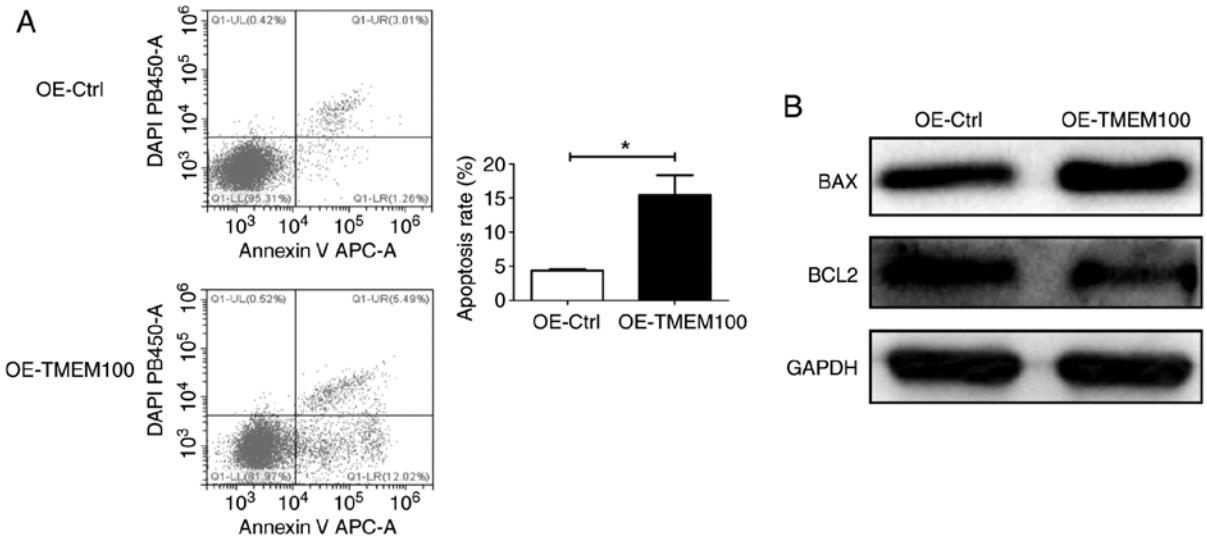

Figure 3. TMEM100 promotes apoptosis in non-small cell lung cancer cells. (A) Flow cytometric analysis of cell apoptosis in A549 cells transfected with TMEM100 overexpression plasmid. (B) Expression level of the apoptosis-related proteins BAX and BCL2 in A549 cells after TMEM100 overexpression. Data are representative of three independent experiments and are presented as the mean ± SD. *P<0.05. TMEM100, transmembrane protein 100; OE, overexpression; Ctrl, control.

and that of the anti-apoptotic protein BCL2 was decreased following TMEM100 overexpression (Fig. 3B). By contrast, knocking down TMEM100 resulted in the opposite effects in H460 cells (Fig. S3A and B). Altogether, these findings indicated that TMEM100 may act as a tumor suppressor that is involved in the promotion of cell apoptosis.

TMEM100 induces autophagy in NSCLC cells via inhibiting the PI3K/AKT signaling pathway. Accumulating evidence has emphasized the importance of autophagy in lung cancer progression (25,26), therefore the effect of TMEM100 on cell autophagy was investigated. The expression of p62 and the transformation of LC3 I to LC3 II, which are essential for autophagy and mainly used as protein markers of autophagy (27), were examined. The results revealed a notable increase in the ratio of LC3 II/LC3 I and a decrease in the expression level of p62 in A549 cells following TMEM100 overexpression (Fig. 4A). Furthermore, knocking down TMEM100 in H460 cells yielded the opposite results (Fig. S4A). In addition, it was observed that TMEM100 overexpression promoted the accumulation of LC3 puncta in A549 cells (Fig. 4B). These results indicated that TMEM100 may induce autophagy in NSCLC cells.

It is well established that the PI3K/AKT signaling pathway is a key signal transduction pathway of autophagy (28,29), therefore the effect of TMEM100 on the PI3K/AKT signaling pathway was investigated. As hypothesized, the level of p-PI3K and p-AKT was decreased after TMEM100 overexpression in A549 cells (Fig. 4C), whereas the expression level of both proteins was markedly increased following knockdown of TMEM100 in H460 cells (Fig. S4B), suggesting that TMEM100 may inhibit the PI3K/AKT signaling pathway. Subsequently, 740Y-P, a PI3K activator, and SC79, an AKT agonist, were used to further examine the association between TMEM100 and the PI3K/AKT signaling pathway and verify whether TMEM100-induced autophagy was associated with the PI3K/AKT signaling pathway. As demonstrated in Fig. 4D and E, pretreatment of A549 cells with 740Y-P and SC79 resulted in an increased activation of PI3K and AKT, respectively, and TMEM100 was observed to attenuate the activatory effects of 740Y-P and SC79. In addition, the ratio of LC3II/LC3I was suppressed after pretreatment with 740Y-P and SC79, and TMEM100 reversed these inhibitory effects (Fig. 4D and E). Pretreatment of H460 cells with LY294002, a PI3K inhibitor, notably reduced the p-PI3K level and increased the LC3 II/LC3 I ratio, whereas TMEM100 knockdown partially reversed the effect of LY294002 (Fig. S4C). Collectively, these findings suggested that TMEM100 may induce autophagy via inhibiting the PI3K/AKT signaling pathway.

Baf-A1 prevents TMEM100-induced autophagy and promotes TMEM100-induced apoptosis. The aforementioned results revealed that TMEM100 induced both apoptosis and autophagy in NSCLC cells. To further explore the relationship between TMEM100-induced autophagy and apoptosis, A549 cells were pretreated with Bafilomycin A1 (Baf-A1), a late autophagy inhibitor, and subsequently transfected with TMEM100 overexpression plasmid or control plasmid. The combination of Baf-A1 treatment and TMEM100 overexpression resulted in increased LC3 II/LC3 I ratio compared with that observed in response to treatment with Baf-A1 or TMEM100 overexpression alone (Fig. 5A), suggesting that TMEM100 may induce autophagy, while Baf-A1 prevented autophagy in A549 cells. In addition, pretreatment with Baf-A1 significantly enhanced apoptosis induced by TMEM100 in A549 cells (Fig. 5B), suggesting that the inhibition of TMEM100-induced autophagy may promote cell death by inducing apoptosis, thereby providing a compensatory mechanism.

Discussion

TMEM100 has been initially identified in the mouse genome and it has been reported to be mainly associated with arterial endothelial differentiation and angiogenesis (5,7). The findings of the present study suggested that TMEM100 may serve as a potential tumor suppressor in NSCLC. The datasets from

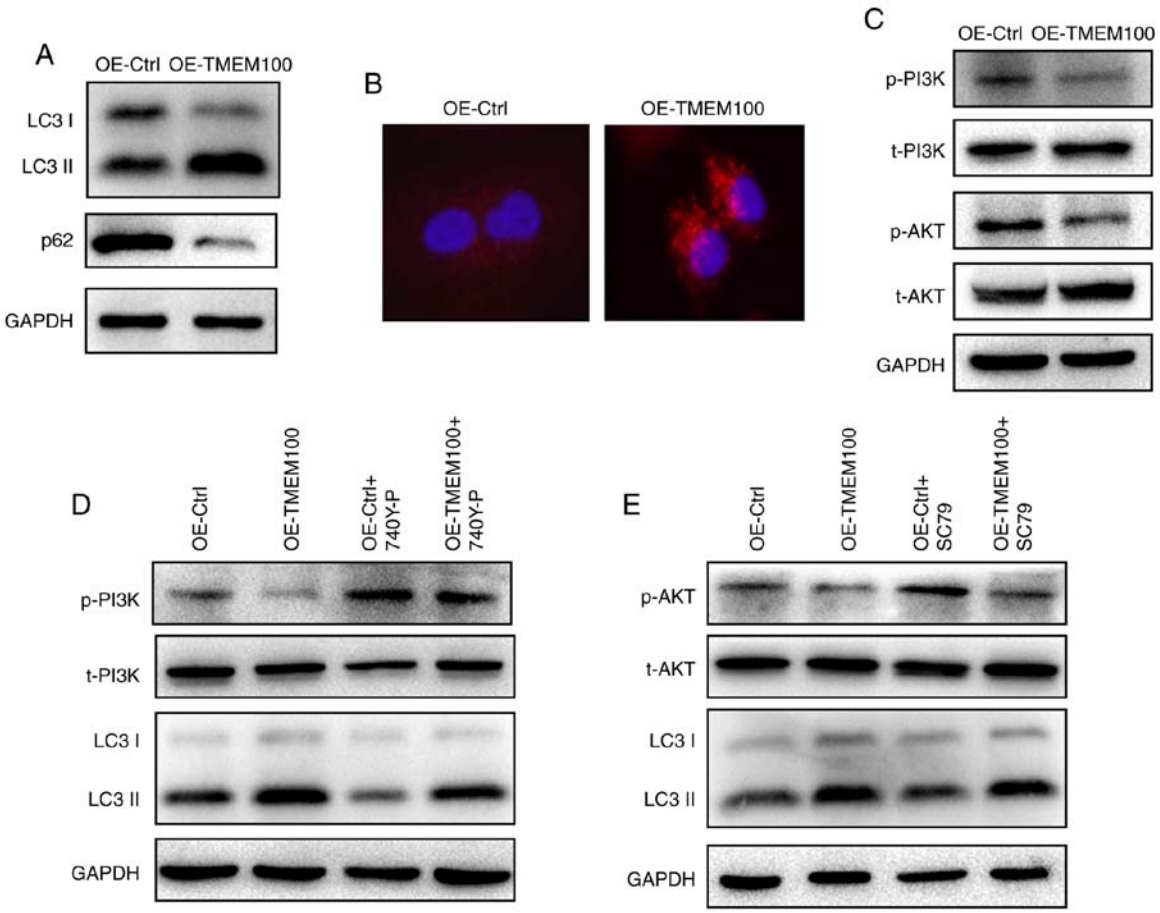

Figure 4. TMEM100 promotes autophagy in non-small cell lung cancer cells via inhibiting the PI3K/AKT signaling pathway. (A) Expression level of the autophagy markers LC3 and p62 in A549 cells upon TMEM100 overexpression. (B) Immunofluorescence staining of LC3 puncta in A549 cells transfected with TMEM100 overexpression plasmid. Red represents the LC3 puncta and blue the cell nucleus. Magnification, x400. (C) Phosphorylation level of PI3K and AKT in A549 cells after TMEM100 overexpression. (D) Expression level of LC3 and phosphorylation level of PI3K in A549 cells transfected with control or TMEM100 overexpression plasmid, with or without treatment with 740Y-P, a PI3K activator. (E) Expression level of LC3 and phosphorylation level of AKT in A549 cells transfected with control or TMEM100 overexpression plasmid, with or without the treatment with SC79, an AKT activator. Data are representative of three independent experiments. TMEM100, transmembrane protein 100; OE, overexpression; Ctrl, control; p, phosphorylated; t, total.

TCGA database were analyzed to determine the expression level of TMEM100 in 533 NSCLC specimens and 59 normal lung tissues. TMEM100 expression level was indicated to be decreased in NSCLC tissues, and it was negatively correlated with the TNM stage and positively correlated with the survival rate of patients, suggesting that TMEM100 may be used as a marker of clinical TNM staging and prognosis in NSCLC. Consistently, the IHC results demonstrated that the expression level of TMEM100 was decreased in NSCLC tissues compared with adjacent non-cancerous tissues. At the cellular level, the expression of TMEM100 in the normal lung epithelial cell line HBE was higher than that in NSCLC cell lines, such as A549, SK-MES-1 and H1299, which was consistent with the results obtained from the CCLE database. Han *et al* (14) compared the expression of TMEM100 in H460, H522, PC9 and A549 cell lines and observed that the expression level of TMEM100 was highest in H460 cells and lowest in A549 cells. However, they selected A549, PC9 and H522 cell lines to demonstrate the antitumor role of TMEM100. Based on the aforementioned results, the present study compared the expression of TMEM100 in H460, HBE, A549, SK-MES-1 and H1299 cell lines and revealed that the expression level of TMEM100 was the highest in H460 and lower in A549 cells. It is worth mentioning that lung adenocarcinoma is the most common type of NSCLC (2) and A549 cell line is a commonly used lung adenocarcinoma cell line. Therefore, H460, HBE and A549 cell lines were selected to demonstrate the antitumor mechanism of TMEM100. Similar to the results of Han *et al* (14), the *in vitro* and *in vivo* experiments of the current study using different cell lines demonstrated the tumor suppressive effects of TMEM100, including the inhibition of cell proliferation and promotion of apoptosis. Collectively, these results revealed that TMEM100 may serve a role as a novel tumor suppressor in NSCLC.

By performing functional studies for TMEM100, the mechanisms underlying the antitumor role of TMEM100 were explored. Autophagy is a highly conserved and finely regulated pathway for maintaining cell homeostasis, which is achieved via inducing lysosomal degradation and recycling of dysfunctional proteins and organelles (30,31). The autophagic process can be divided into four steps: Induction, elongation, transportation to lysosomes and degradation (32). Autophagy can be activated by various type of stress, such as starvation, hypoxia and radiation exposure (33). Notably, the dysregulation of autophagy has been identified as a pathogenic feature of cancer (34,35). Previous studies have reported a dual role for autophagy in tumorigenesis.

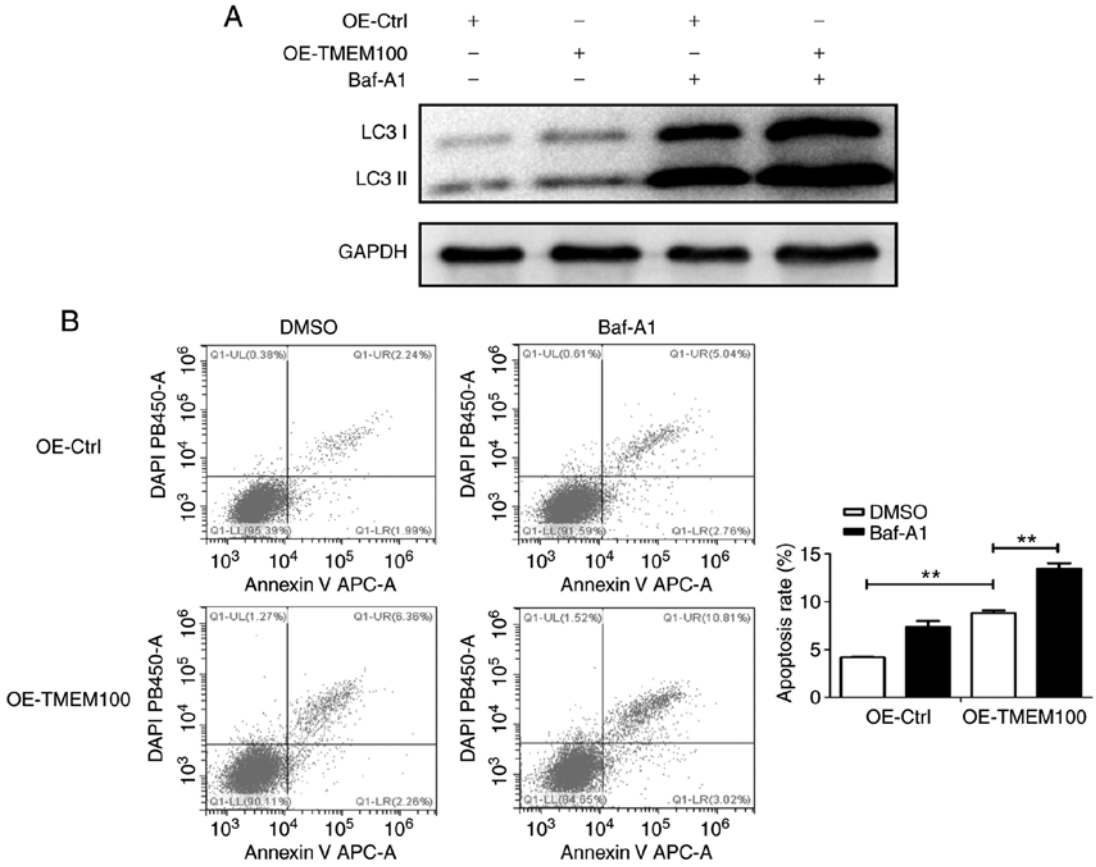

Figure 5. Baf-A1 promotes TMEM100-induced apoptosis in A549 cells. (A) Expression level of LC3 in A549 cells transfected with control or TMEM100 overexpression plasmid, with or without the treatment with Baf-A1, an autophagy inhibitor. (B) Flow cytometric analysis of cell apoptosis in A549 cells transfected with control or TMEM100 overexpression plasmid, with or without the treatment with Baf-A1. Data are representative of three independent experiments and are presented as the mean ± SD. **P<0.01. TMEM100, transmembrane protein 100; OE, overexpression; Ctrl, control; Baf-A1, bafilomycin A1.

For instance, cancer cells have been demonstrated to induce autophagy under stressful or nutrition-deprived conditions to promote cell survival (36), but excessive or constitutive activation of autophagy has been indicated to result in cancer cell death (37). In NSCLC, Nrf2 has been demonstrated to promote tumorigenesis via activating autophagy (22). In Ras-transformed cells, autophagy has been indicated to facilitate tumor cell survival via maintaining aerobic glycolysis and the tricarboxylic acid cycle for cellular energy demands (38). The antitumor effect of autophagy has also been reported in NSCLC; for instance, autophagy induced by Licarin A from *Myristica fragrans* has been revealed to promote cell death in NSCLC cell lines (32). Interestingly, the deletion of Atg7 has been indicated to accelerate tumor development initially, but suppress tumor progression in the later stages (20), demonstrating the paradoxical role of autophagy in cancer even within the same model. To date, there have been no reports elucidating the association between TMEM100 and autophagy, to the best of our knowledge. In the present study, the effect of TMEM100 on the autophagy of NSCLC cells was investigated. The results revealed that TMEM100 could induce autophagy by increasing the ratio of LC3 II /LC3 I and decreasing the expression level of p62. Moreover, LC3 puncta were observed to increase upon TMEM100 overexpression. Previous studies have demonstrated that a tumor suppressor, such as p53 or PTEN, inhibited tumor growth by inducing autophagy (39,40), which are in line with the results of the present study.

There are several signaling pathways underlying the regulation of cell autophagy, including the PI3K/AKT, Beclin-1 and ERK1/2 signaling pathways (41-44). Accumulating evidence has suggested that the PI3K/AKT signaling pathway is a critical mediator in the regulation of cell autophagy (41-44). It has been demonstrated that the deactivation of the PI3K/AKT signaling pathway may result in autophagy induction (45). In addition, the dysregulation of the PI3K/AKT signaling pathway has been closely associated with tumor development, metastasis and apoptosis in lung cancer (45). Based on these findings, it was hypothesized that TMEM100 may stimulate autophagy via blocking the PI3K/AKT signaling pathway. This hypothesis was supported by the decreased level of p-PI3K and p-AKT upon TMEM100 overexpression. Conversely, the activation of PI3K and AKT by 740Y-P and SC79 significantly reduced the expression level of LC3 II, which was increased by the overexpression of TMEM100. These findings validated that TMEM100 may activate autophagy via inhibiting the PI3K/AKT signaling pathway. To further investigate the mechanisms of TMEM100 function associated with NSCLC progression, whole transcriptome sequencing analysis was performed in A549 cells transfected with TMEM100 overexpression plasmid and empty plasmid. The sequencing results demonstrated that CHOP, GADD34, GRP78, XBP1 and other genes involved in endoplasmic reticulum stress (ERS) were downregulated after TMEM100 overexpression, which was confirmed by RT-qPCR and western blotting (data not shown).

Future studies will be focused on the role and mechanism of function of TMEM100 in the regulation of ERS and the association between ERS and TMEM100-induced autophagy.

Recently, autophagy was termed type II programmed cell death (46). In certain cases, autophagy and apoptosis are interconnected, but their association has not been fully investigated. Previous studies have supported the relevance of the interplay between autophagy and apoptosis (37,47). It has been reported that both autophagy and apoptosis served important roles in lung cancer progression (48), and their synergistic actions promoted cell death. For instance, Licarin A, which was derived from *Myristica fragrans*, activated autophagy and apoptosis, thereby resulting in the death of NSCLC cells (32). HSP90 inhibitor DPB has been also indicated to inhibit A549 cell growth by inducing apoptosis and autophagy (49). In the present study, it was revealed that TMEM100 could promote both apoptosis and autophagy, and inhibition of autophagy by Baf-A1 notably enhanced TMEM100-induced apoptosis. The results were consistent with a previous study in gastric cancer, which demonstrated that the tumor suppressor XIAP-associated factor 1 (XAF1) could induce autophagic cell death, whilst 3-MA treatment enhanced XAF1-induced apoptosis (43). These results indicated that TMEM100-induced autophagy and apoptosis may be complementary events to ensure cell death.

In conclusion, the present study validated the role of TMEM100 as a tumor suppressor in NSCLC. TMEM100 was demonstrated to inhibit cell proliferation and promote cell death by inducing apoptosis and autophagy. To the best of our knowledge, the current study was the first to demonstrate that TMEM100 could activate autophagy in NSCLC cells and to indicate that the inhibition of the PI3K/AKT signaling pathway may be one of the mechanisms underlying TMEM100-induced autophagy. Furthermore, the inhibition of autophagy by Baf-A1 was indicated to increase the proportion of apoptotic cells, suggesting a complementary role of TMEM100-induced apoptosis and autophagy. Therefore, the present study revealed a novel mechanism by which TMEM100 may inhibit tumor progression.

Acknowledgements

Not applicable.

Funding

The present study was supported by National Natural Science Foundation of China (grant no. csfc81373151) and Chongqing Science and Technology Commission (grant no. cstc2018jcyjAX0257).

Availability of data and materials

The datasets used and/or analyzed during the current study are available from the corresponding author on reasonable request.

Authors' contributions

QH and YH conceived and designed the research. QH, YD, YZ, ZD, XZ, ZW, RA performed the experiments and analyzed the data. QH and YH wrote the manuscript. ZD and YH interpreted the data and corrected the manuscript. QH and YH confirm the authenticity of the raw data. All authors read and approved the final manuscript.

Ethics approval and consent to participate

The present study was approved by Ethics and Research Committees of Chongqing Medical University (Chongqing, China). All animal experiments were approved by the Institutional Animal Care and Use Committee of Chongqing Medical University (Chongqing, China).

Patient consent for publication

Not applicable.

Competing interests

The authors declare that they have no competing interests.

References

1. Siegel RL, Miller KD and Jemal A: Cancer statistics, 2017. CA Cancer J Clin 67: 7-30, 2017.
2. Herbst RS, Heymach JV and Lippman SM: Lung cancer. N Engl J Med 359: 1367-1380, 2008.
3. Lemjabbar-Alaoui H, Hassan OU, Yang YW and Buchanan P: Lung cancer: Biology and treatment options. Biochim Biophys Acta 1856: 189-210, 2015.
4. Herbst RS, Morgensztern D and Boshoff C: The biology and management of non-small cell lung cancer. Nature 533: 446-454, 2018.
5. Kawai J, Shinagawa A, Shibata K, Yoshino M, Itoh M, Ishii Y, Arakawa T, Hara A, Fukunishi Y, Konno H, *et al*: Functional annotation of a full-length mouse cDNA collection. Nature 409: 685-690, 2001.
6. Moon EN, Kim MJ, Ko KS, Kim YS, Seo J, Oh SP and Lee YJ: Generation of mice with a conditional and reporter allele for Tmem100. Genesis 48: 673-678, 2010.
7. Somekawa S, Imagawa K, Hayashi H, Sakabe M, Ioka T, Sato GE, Inada K, Iwamoto T, Mori T, Uemura S, *et al*: Tmem100, an ALK1 receptor signaling-dependent gene essential for arterial endothelium differentiation and vascular morphogenesis. Proc Natl Acad Sci USA 109: 12064-12069, 2012.
8. Moon EH, Kim YS, Seo J, Lee YJ and Oh SP: Essential role for TMEM100 in vascular integrity but limited contributions to the pathogenesis of hereditary haemorrhagic telangiectasia. Cardiovasc Res 105: 353-360, 2015.
9. Yamazaki T, Muramoto M, Okitsu O, Morikawa N and Kita Y: Discovery of a novel neuroprotective compound, AS1219164, by high-throughput chemical screening of a newly identified apoptotic gene marker. Eur J Pharmacol 669: 7-14, 2011.
10. Eisenman ST, Gibbons SJ, Singh RD, Bernard CE, Wu J, Sarr MG, Kendrick ML, Larson DW, Dozois EJ, Shen KR and Farrugia G: Distribution of TMEM100 in the mouse and human gastrointestinal tract-a novel marker of enteric nerves. Neuroscience 240: 117-128, 2013.
11. Weng HJ, Patel KN, Jeske NA, Bierbower SM, Zou W, Tiwari V, Zheng Q, Tang Z, Mo GC, Wang Y, *et al*: Tmem100 is a regulator of TRPA1-TRPV1 complex and contributes to persistent pain. Neuron 85: 833-846, 2015.
12. Frullanti E, Colombo F, Falvella FS, Galvan A, Noci S, De Cecco L, Incarbone M, Alloisio M, Santambrogio L, Nosotti M, *et al*: Association of lung adenocarcinoma clinical stage with gene expression pattern in noninvolved lung tissue. Int J Cancer 131: E643-E648, 2012.
13. Ou D, Yang H, Hua D, Xiao S and Yang L: Novel roles of TMEM100: Inhibition metastasis and proliferation of hepatocellular carcinoma. Oncotarget 6: 17379-17390, 2015.
14. Han Z, Wang T, Han S, Chen Y, Chen T, Jia Q, Li B, Li B, Wang J, Chen G, *et al*: Low-expression of TMEM100 is associated with poor prognosis in non-small-cell lung cancer. Am J Transl Res 9: 2567-2578, 2017.

15. Yang ZJ, Chee CE, Huang S and Sinicrope FA: The role of autophagy in cancer: Therapeutic implications. Mol Cancer Ther 10: 1533-1541, 2011.
16. Arroyo DS, Gaviglio EA, Peralta Ramos JM, Bussi C, Rodriguez-Galan MC and Iribarren P: Autophagy in inflammation, infection, neurodegeneration and cancer. Int Immunopharmacol 18: 55-65, 2014.
17. Ding ZB, Shi YH, Zhou J, Qiu SJ, Xu Y, Dai Z, Shi GM, Wang XY, Ke AW, Wu B and Fan J: Association of autophagy defect with a malignant phenotype and poor prognosis of hepatocellular carcinoma. Cancer Res 68: 9167-9175, 2008.
18. Zhang H, Zhang Y, Zhu X, Chen C, Zhang C, Xia Y, Zhao Y, Andrisani O and Kong L: DEAD box protein 5 inhibits liver tumorigenesis by stimulating autophagy via interaction with p62/SQSTM1. Hepatology 69: 1046-1063, 2019.
19. Guo JY, Teng X, Laddha SV, Ma S, Van Nostrand SC, Yang Y, Khor S, Chan CS, Rabinowitz JD and White E: Autophagy provides metabolic substrates to maintain energy charge and nucleotide pools in Ras-driven lung cancer cells. Genes Dev 30: 1704-1717, 2016.
20. Strohecker AM, Guo JY, Karsli-Uzunbas G, Price SM, Chen GJ, Mathew R, McMahon M and White E: Autophagy sustains mitochondrial glutamine metabolism and growth of BrafV600E-driven lung tumors. Cancer Discov 3: 1272-1285, 2013.
21. Poillet-Perez L, Xie X, Zhan L, Yang L, Sharp DW, Hu ZS, Su X, Maganti A, Jiang C, Lu W, *et al*: Autophagy maintains tumour growth through circulating arginine. Nature 563: 569-573, 2018.
22. Wang J, Liu Z, Hu T, Han L, Yu S, Yao Y, Ruan Z, Tian T, Huang T, Wang M, *et al*: Nrf2 promotes progression of non-small cell lung cancer through activating autophagy. Cell Cycle 16: 1053-1062, 2017.
23. Cai J, Li R, Xu X, Zhang L, Lian R, Fang L, Huang Y, Feng X, Liu X, Li X, *et al*: CK1α suppresses lung tumour growth by stabilizing PTEN and inducing autophagy. Nat Cell Biol 20: 465-478, 2018.
24. Livak KJ and Schmittgen TD: Analysis of relative gene expression data using real-time quantitative PCR and the 2(-Delta Delta C(T)) method. Methods 25: 402-408, 2001.
25. Karsli-Uzunbas G, Guo JY, Price S, Teng X, Laddha SV, Khor S, Kalaany NY, Jacks T, Chan CS, Rabinowitz JD and White E: Autophagy is required for glucose homeostasis and lung tumor maintenance. Cancer Discov 4: 914-927, 2014.
26. Rao S, Yang H, Penninger JM and Kroemer G: Autophagy in non-small cell lung carcinogenesis: A positive regulator of anti-tumor immunosurveillance. Autophagy 10: 529-531, 2014.
27. Klionsky DJ, Abdelmohsen K, Abe A, Abedin MJ, Abeliovich H, Acevedo Arozena A, Adachi H, Adams CM, Adams PD, Adeli K, *et al*: Guidelines for the use and interpretation of assays for monitoring autophagy (3rd edition). Autophagy 12: 1-222, 2016.
28. Fan S, Zhang B, Luan P, Gu B, Wan Q, Huang X, Liao W and Liu J: PI3K/AKT/mTOR/p70S6K pathway is involved in Aβ25-35-induced autophagy. Biomed Res Int 2015: 161020, 2015.
29. Hou X, Hu Z, Xu H, Xu J, Zhang S, Zhong Y, He X and Wang N: Advanced glycation endproducts trigger autophagy in cadiomyocyte via RAGE/PI3K/AKT/mTOR pathway. Cardiovasc Diabetol 13: 78, 2014.
30. Dikic I, Johansen T and Kirkin V: Selective autophagy in cancer development and therapy. Cancer Res 70: 3431-3434, 2010.
31. Janku F, McConkey DJ, Hong DS and Kurzrock R: Autophagy as a target for anticancer therapy. Nat Rev Clin Oncol 8: 528-539, 2011.
32. Maheswari U, Ghosh K and Sadras SR: Licarin A induces cell death by activation of autophagy and apoptosis in non-small cell lung cancer cells. Apoptosis 23: 210-225, 2018.
33. Kimura S, Noda T and Yoshimori T: Dissection of the autophagosome maturation process by a novel reporter protein, tandem fluorescent-tagged LC3. Autophagy 3: 452-460, 2007.
34. White E: The role for autophagy in cancer. J Clin Invest 125: 42-46, 2015.
35. Lavandero S, Chiong M, Rothermel BA and Hill JA: Autophagy in cardiovascular biology. J Clin Invest 125: 55-64, 2015.
36. Guo XL, Li D, Sun K, Wang J, Liu Y, Song JR, Zhao QD, Zhang SS, Deng WJ, Zhao X, *et al*: Inhibition of autophagy enhances anticancer effects of bevacizumab in hepatocarcinoma. J Mol Med (Berl) 91: 473-483, 2013.
37. Zhang P, Zheng Z, Ling L, Yang X, Zhang N, Wang X, Hu M, Xia Y, Ma Y, Yang H, *et al*: w09, a novel autophagy enhancer, induces autophagy-dependent cell apoptosis via activation of the EGFR-mediated RAS-RAF1-MAP2K-MAPK1/3 pathway. Autophagy 13: 1093-1112, 2017.
38. White E: Deconvoluting the context-dependent role for autophagy in cancer. Nat Rev Cancer 12: 401-410, 2012.
39. Abida WM and Gu W: p53-dependent and p53-independent activation of autophagy by ARF. Cancer Res 68: 352-357, 2008.
40. Arico S, Petiot A, Bauvy C, Dubbelhuis PF, Meijer AJ, Codogno P and Ogier-Denis E: The tumor suppressor PTEN positively regulates macroautophagy by inhibiting the phosphatidylinositol 3-kinase/protein kinase B pathway. J Biol Chem 276: 35243-35246, 2001.
41. Liu J, Wang X, Zheng M and Luan Q: Lipopolysaccharide from Porphyromonas gingivalis promotes autophagy of human gingival fibroblasts through the PI3K/Akt/mTOR signaling pathway. Life Sci 211: 133-139, 2018.
42. Qi HY, Qu XJ, Liu J, Hou KZ, Fan YB, Che XF and Liu YP: Bufalin induces protective autophagy by Cbl-b regulating mTOR and ERK signaling pathways in gastric cancer cells. Cell Bio Int 43: 33-43, 2019.
43. Sun PH, Zhu LM, Qiao MM, Zhang YP, Jiang SH, Wu YL and Tu SP: The XAF1 tumor suppressor induces autophagic cell death via upregulation of Beclin-1 and inhibition of Akt pathway. Cancer Lett 310: 170-180, 2011.
44. Li YC, He SM, He ZX, Li M, Yang Y, Pang JX, Zhang X, Chow K, Zhou Q, Duan W, *et al*: Plumbagin induces apoptotic and autophagic cell death through inhibition of the PI3K/Akt/mTOR pathway in human non-small cell lung cancer cells. Cancer Lett 344: 239-259, 2014.
45. Schuurbiers OC, Kaanders JH, van der Heijden HF, Dekhuijzen RP, Oyen WJ and Bussink J: The PI3-K/AKT-pathway and radiation resistance mechanisms in non-small cell lung cancer. J Thorac oncol 4: 761-767, 2009.
46. Cao L, Walker MP, Vaidya NK, Fu M, Kumar S and Kumar A: Cocaine-mediated autophagy in astrocytes involves sigma 1 receptor, PI3K, mTOR, Atg5/7, Beclin-1 and induces type II programmed cell death. Mol Neurobiol 53: 4417-4430, 2016.
47. Kaminskyy VO, Piskunova T, Zborovskaya IB, Tchevkina EM and Zhivotovsky B: Suppression of basal autophagy reduces lung cancer cell proliferation and enhances caspase-dependent and -independent apoptosis by stimulating ROS formation. Autophagy 8: 1032-1044, 2012.
48. Liu G, Pei F, Yang F, Li L, Amin AD, Liu S, Buchan JR and Cho WC: Role of autophagy and apoptosis in non-small-cell lung cancer. Int J Mol Sci 18: 367, 2017.
49. Zhao Y, Li K, Zhao B and Su L: HSP90 inhibitor DPB induces autophagy and more effectively apoptosis in A549 cells combined with autophagy inhibitors. In Vitro Cell Dev Biol Anim 55: 349-354, 2019.